Catalysis Science & Technology

Silica-decorated Ni–Zn alloy as a highly active and selective catalyst for acetylene semihydrogenation

Journal:	*Catalysis Science & Technology*
Manuscript ID	CY-COM-04-2021-000709.R1
Article Type:	Communication
Date Submitted by the Author:	05-May-2021
Complete List of Authors:	Simanulang, Wiyanti; Hokkaido University, Institute for Catalysis Ma, Jiamin; Hokkaido University, Institute for Catalysis Shimizu, Ken-ichi; Hokkaido University, Institute for Catalysis Furukawa, Shinya; Hokkaido University, Institute for Catalysis

COMMUNICATION

Silica-decorated Ni–Zn alloy as a highly active and selective catalyst for acetylene semihydrogenation

Wiyanti F. Simanullang,[a†] Jiamin Ma,[a†] Ken-ichi Shimizu,[a,b] Shinya Furukawa,[*a,b,c]

Received 00th January 20xx,
Accepted 00th January 20xx

DOI: 10.1039/x0xx00000x

A silica-decoration methodology was adopted to Ni–Zn alloy for developing active and selective acetylene semihydrogenation. Ni–Zn alloy nanoparticles on SiO_2 were further decorated by additional silica, which significantly increased the acetylene conversion (15%–97%) without lowering ethylene selectivity (ca. 80%) at 200°C.

Precious metals, such as Pd and Pt, are highly active catalysts for hydrogenation and dehydrogenation. However, their high cost hampers the widespread application of large-scale chemical processes. Thus, it is essential to develop efficient catalytic systems based on cheap and earth-abundant elements.[1–8] Although Ni-based catalysts have been regarded as promising noble metal alternatives because of their much lower cost, the catalytic activity is unsatisfactory compared with those of Pt- and Pd-based materials.[9] Therefore, developing highly active Ni-based catalysts for (de)hydrogenation reactions is attractive in the field of pure and applied chemistry.

Chemical modification of Ni-based alloy has been a possible methodology for this purpose. For instance, the base-extraction of Al from Ni–Al alloy is a well-known method to afford porous and active Ni catalysts (Raney®-Ni) for hydrogenation reactions. Recently, Abe et al. reported that "Ni-based rooted catalyst" was obtained from Ni_3Y alloy by reaction with CO and O_2, which was stable for dry reforming of methane.[10]

We reported another efficient method, i.e., surface dealloying of Ni–Si intermetallics. The surface of Ni–Si intermetallics was transformed into a unique structure, where small Ni clusters (2–3 nm) were embedded in the SiO_2 matrix. This material was more active than monometallic Pd in benzene hydrogenation.[11] Recently, we extended these interesting Ni structures from the bulk material to supported system using additional silica-decoration to conventional Ni nanoparticles on SiO_2 support. The silica-decoration changed the morphology of Ni nanoparticles from spherical to rough and anisotropic, where the number of step sites significantly increased (Scheme 1, left) and the catalytic activities in alkane (de)hydrogenation and aromatic hydrogenation were enhanced.[12]

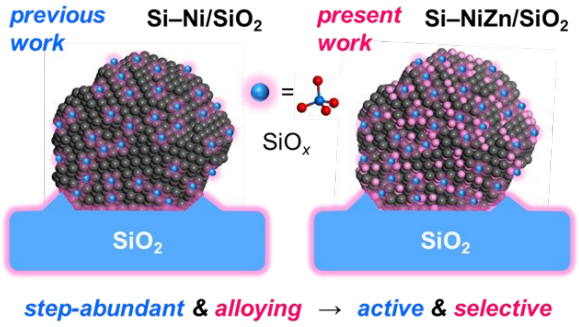

Scheme 1. Catalyst design concepts in the previous ($Si–Ni/SiO_2$) and current studies ($Si–Ni–Zn/SiO_2$). The silica-decoration to Ni nanoparticles on SiO_2 makes the morphology rough and anisotropic, where a substantial number of step sites are present. Gray: Ni, magenta: Zn, cyan: silica.

Next, we focused on developing a highly active and "selective" catalyst for semihydrogenation of alkynes. Activity and selectivity are in a tradeoff relationship for selective hydrogenation because higher activity tends to induce undesired over hydrogenation. Thus, achieving high activity and selectivity has been regarded as a challenging task in catalytic chemistry. As a model reaction, we focused on acetylene semihydrogenation since it is an industrially important process for purifying crude ethylene with trace acetylene for ethylene polymerization;[13–15] it is also of interest to researchers on fundamental surface chemistry.[16–18] Ni–Zn alloy is a highly selective catalyst for acetylene semihydrogenation into ethylene because of the lowered d-band center, which promotes ethylene desorption.[19, 20] However, the catalytic activity of Ni–Zn alloy was much lower than precious-metal-based catalysts such as Pd–Zn.[21, 22] In this study, we attempted

[a] *Institute for Catalysis, Hokkaido University, N21 W10, Kita-ku, Sapporo, 001-0021, Japan. E-mail: furukawa@cat.hokudai.ac.jp*
[b] *Elements Strategy Initiative for Catalysts and Batteries, Kyoto University, Katsura, Kyoto 615-8520, Japan*
[c] *Japan Science and Technology Agency, PRESTO, Chiyoda-ku, Tokyo, 102-0076*
† These authors equally contributed.
Electronic Supplementary Information (ESI) available: [details of any supplementary information available should be included here]. See DOI: 10.1039/x0xx00000x

to improve the catalytic activity of Ni–Zn alloy in acetylene semihydrogenation without lowering its selectivity using the silica-decoration method (Scheme 1, right). We report a highly active and selective Ni-based catalyst for acetylene semihydrogenation and the synergy of alloying and the silica-decoration effects on catalysis.

The catalyst preparation was simple; Ni–Zn alloy nanoparticles on silica support (Ni–Zn/SiO_2, Ni: 2 wt.%, Ni/Zn = 1) were prepared by a pore-filling co-impregnation method using a mixed aqueous solution of Ni and Zn nitrates, followed by drying (80°C), calcination (500°C), and reduction (500°C). Silica-decorated Ni–Zn (Si–Ni–Zn/SiO_2, Ni/Si = 4) was prepared in a similar manner using thus-prepared Ni–Zn/SiO_2 and an ethanol solution of triphenylsilanol, $(C_6H_5)_3SiOH$ (see Supporting Information for details). The organic silanol is transformed into silica during the calcination process.

The X-ray diffraction (XRD) patterns of Ni–Zn/SiO_2 and Si–Ni–Zn/SiO_2 (Fig. S1) showed that the 3:1 Ni–Zn solid-solution alloy phase was formed for both catalysts. The crystallite size estimated from Scherrer's equation was about 3 nm in each case. This result showed that the silica-decoration did not change the size and degree of alloying of Ni–Zn nanoparticles. Then, we conducted high angle annular dark field scanning transmission electron microscopy–energy dispersive X-ray spectroscopy (HAADF-STEM-EDX) analysis for Si–Ni–Zn/SiO_2 catalyst. The particle size ranged from 2 to 6 nm, and the volume-weighted average was 3.9 nm (Figs. 1(a–c)), which is consistent with the crystallite size estimated by XRD. The high-resolution HAADF-STEM image of a single nanoparticle showed the atomic arrangement of an fcc crystal viewed along the [001] direction (Fig. 1(d)). The elemental map indicates that the nanoparticles consist of Ni and Zn (Figs. 1(e) and (f)). Based on these results, it can be concluded that the 3:1 solid-solution alloy of Ni–Zn was formed as small nanoparticles on SiO_2.

The temperature-programmed reduction by H_2 (H_2-TPR) was conducted for Ni–Zn/SiO_2 and Si–Ni–Zn/SiO_2 to compare the reducibility of each catalyst (Fig. S2). For undecorated Ni–Zn, intense reduction peaks appeared at 246°C and 316°C, which is attributed to the reduction of Ni and Zn, respectively.[23, 24] The reduction peaks appearing at more than 500°C may be assigned to Zn oxide species strongly bound on SiO_2. The appearance of this reduction indicates that not all the Zn species was reduced at 500°C (temperature for catalyst preparation and pretreatment) and the presence of Zn oxide on the catalyst. It is consistent with the 3:1 alloy phase formed even though the Ni/Zn fed ratio was 1. For Si–Ni–Zn, these reduction peaks shifted to higher temperatures (246°C→262°C, 306°C; 316°C→406°C; 541°C→763°C). It indicates that the reduction of Ni and Zn is inhibited by the additional silica species, and that there is some chemical interaction between metals (Ni and Zn) and additional silica species. This result also suggests that the Ni–Zn alloy nanoparticles have close contact with the additional silica species. Then, we performed Fourier-transform infrared (FT-IR) analysis with CO adsorption at −196°C to characterize the surface structure. As shown in Fig. 2, Ni–Zn/SiO_2 and Si–Ni–Zn/SiO_2 showed adsorption bands at 2065 cm^{-1} and 2018 cm^{-1}, respectively, both of which are assignable to CO linearly

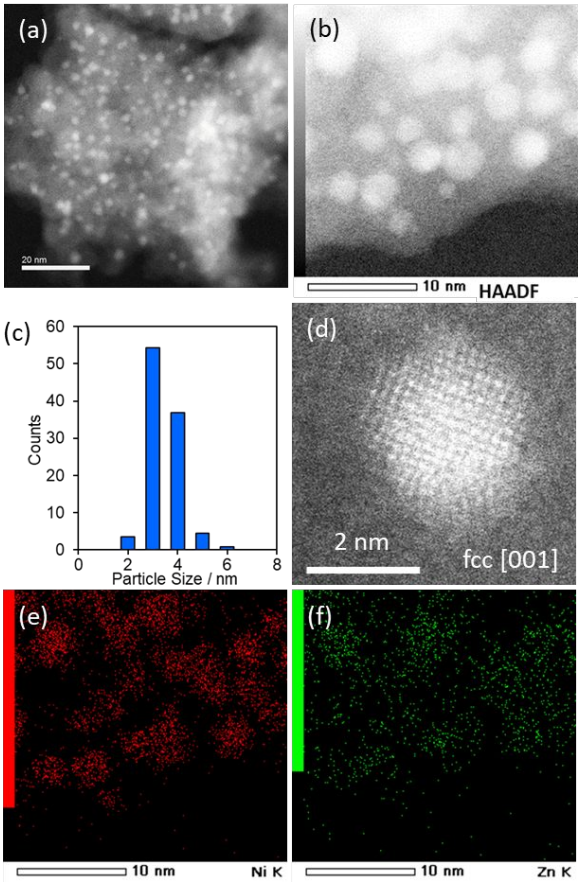

Fig. 1. HAADF-STEM-EDX of Si–Ni–Zn on SiO_2 support. (a) and (b) HAADF-STEM image of Si–Ni–Zn/SiO_2 (Ni:Zn = 1:1) (c) size distribution of the nanoparticle (d) high resolution of HAADF-STEM and elemental maps of (e) Ni and (f) Zn acquired using EDX.

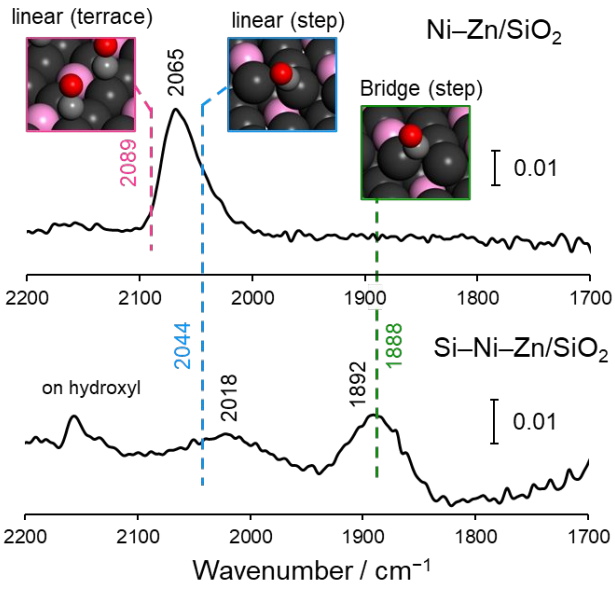

Fig. 2. FT-IR spectra of CO adsorbed on Ni–Zn/SiO_2 and Si–Ni–Zn/SiO_2 measured at −196°C. Inset figures indicate the optimized structure of linear and bridge CO on the terrace site of $Ni_3Zn(111)$ and the step site of $Ni_3Zn(111)$ calculated by DFT. The corresponding theoretical frequencies of CO stretching vibration were indicated as vertical dashed lines and colored values.

adsorbed on Ni alloyed with Zn.[25] We recently reported a similar deviation in the peak position of linear CO upon silica-decoration for monometallic Ni/SiO_2, where a DFT calculation indicated that the band at lower wavenumber can be assignable to CO adsorbed on the step Ni site.[11] Likewise, in this study, we calculated the theoretical vibrational frequency of adsorbed CO on Ni_3Zn(111) and Ni_3Zn(211) (see ESI for computational details).

The calculated frequency of linear CO on the step Ni sites was 2044 cm^{-1}, which was redshifted by 45 cm^{-1} to that on the terrace site (2089 cm^{-1}). Thus, the DFT calculation well reproduced the experimental redshift of 47 cm^{-1} and supports that step Ni sites are mainly present on the surface of Si–Ni–Zn/SiO_2. Ni–Zn/SiO_2 did not show bridge CO as reported in literature, which is due to the ensemble effect by Zn. In contrast, bridge CO was observed at 1892 cm^{-1} on Si–Ni–Zn/SiO_2. The DFT calculation for the bridge CO at the step Ni site well reproduced the experimental value (1888 cm^{-1}), suggesting that the bridge adsorption mode is allowed for the step site even on Ni–Zn alloy surface.

Finally, we tested the catalytic performances of the prepared Ni-based catalysts in acetylene semihydrogenation. Fig. 3 shows acetylene conversion and ethylene selectivity for the tested catalysts.

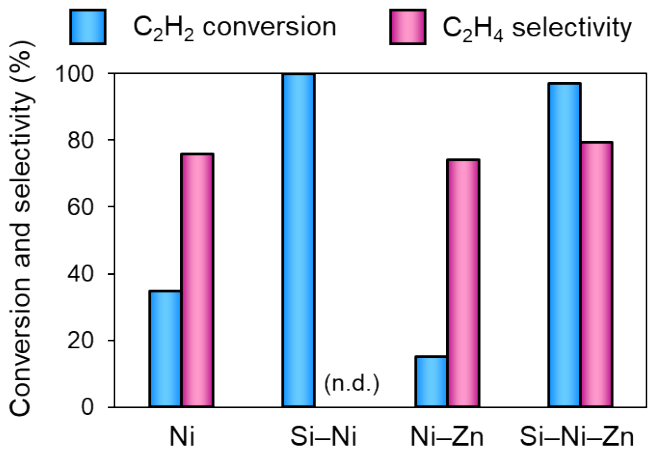

Fig. 3. (a) Catalytic performance of Ni-based catalysts in acetylene semihydrogenation (Ni loading: 2wt%, Ni:Si = 1:4, T = 130°C for Ni and Si–Ni, 200°C for Ni–Zn and Si–Ni–Zn.

For better comparison, control experiments using monometallic Ni with and without silica-decoration (Ni/SiO_2 and Si–Ni/SiO_2) were also conducted. Conventional Ni/SiO_2 showed good selectivity at a low conversion level. The silica-decoration to monometallic Ni significantly improved the acetylene conversion from 37% to 100% (130°C). However, no ethylene was obtained due to excess over hydrogenation to ethane, which is widely known for monometallic Ni. Thus, the silica-decoration methodology alone does not apply to selective hydrogenation systems. Ni–Zn/SiO_2 showed high ethylene selectivity as reported in the literature,[19] much higher temperature (200°C) was needed to obtain an acetylene conversion comparable to that for Ni/SiO_2. However, Si–Ni–Zn/SiO_2 exhibited much higher acetylene conversion (97%) and good ethylene selectivity (80%). Thus, the acetylene conversion was excellently improved without lowering ethylene selectivity. We also confirmed that Si–Ni–Zn/SiO_2 showed much higher acetylene conversion than Ni–Zn/SiO_2 at various temperatures (150°C–200°C, Fig. S3) and its catalytic performance was stable at least for 6 h (Fig. S4). These results showed that the silica-decoration method applies to alkyne hydrogenation and is compatible with the alloying effect on high selectivity. Fig. 4 summarizes the catalytic performances of various Ni-based catalyst for acetylene semihydrogenation (see ESI Table S1 for more details).

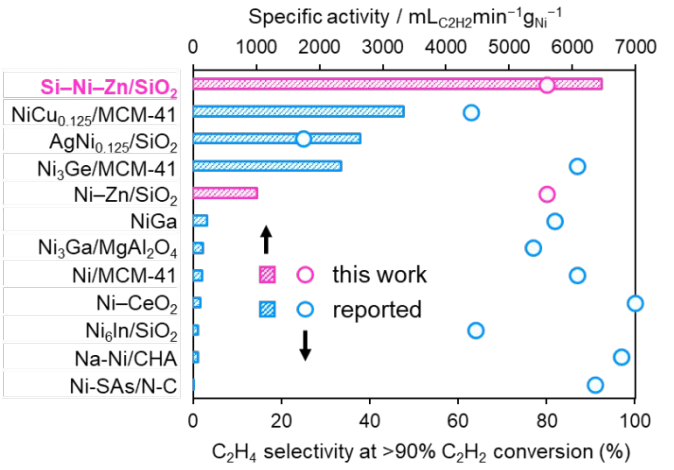

Fig. 4. Summary of the catalytic performance of various Ni-based catalysts in acetylene semihydrogenation. For Ni_3Ge/MCM-41 and Ni–Zn/SiO_2, the specific activities at 30% and 15% conversions are shown, respectively.

Si–Ni–Zn/SiO_2 exhibited twice higher specific activity (mL acetylene converted per min per gram Ni) than the highest ever reported,[26] which highlights the outstanding high catalytic activity and promotion effect of silica-decoration. In the previous study, we demonstrated that silica-decoration methodology was valid for alkane dehydrogenation and aromatic hydrogenation. We showed that this catalyst design concept might be valid for various catalytic systems. Besides, we obtained the Arrhenius-type plots for this reaction, where the apparent activation energy was almost similar with and without silica-decoration (Fig. S5). It indicates that the hydrogenation ability (apparent activation energy and the resulting reaction rate) of one active site is not changed by the silica-decoration. Thus, the enhanced catalytic activity may be due to the increase in the number of active sites (probably, step sites) induced by silica-modification. Here, one may think that the silica decoration may decrease the number of active step sites. However, note that there is almost no active step site on unmodified Ni–Zn/SiO_2, whereas the step sites remain as active sites on Si–Ni–Zn/SiO_2, as evidenced by the FT-IR study. Therefore, the number of active step sites on Si–Ni–Zn/SiO_2 should be larger than that on Ni–Zn/SiO_2, which is the origin of the enhanced catalytic activity. What is important is that the step site cannot be present alone because it is unstable in the absence of the silica-decoration. Although some of the step

sites are needed to be occupied with the additional silica for the stabilization of the step-abundant structure, there is no need to completely cover all the step sites. One may also think that why high selectivity was retained even with the significantly improved catalytic activity, because higher activity typically results in lower selectivity due to over hydrogenation. A possible interpretation might be the geometric effect of the step site on selectivity. Compared with C_2H_2, C_2H_4 molecule has larger steric hindrance. Besides, hydrogen diffusion is regulated at the step site. Therefore, hydrogen attack to C_2H_4 at the step site may be more geometrically supressed compared with that to C_2H_2. Thus, the combination of the high activity and geometric restriction of the step site may enable the highly active and selective semihydrogenation of acetylene.

In summary, we applied the silica-decoration method to Ni–Zn alloy nanoparticles supported on silica. The silica-decoration significantly improved the catalytic activity of Ni–Zn alloy in acetylene semihydrogenation without lowering the ethylene selectivity. The catalyst design concept based on silica-decoration would apply to various catalytic systems to improve catalytic performance.

Acknowledgements

This work was supported by JSPS KAKENHI (Grant Numbers 17H01341, 17H04965, and 20H02517) and by the Collaborative Research Projects of Laboratory for Materials and Structures, Institute of Innovative Research, Tokyo Institute of Technology, as well as by the JST CREST (JPMJCR17J3) and PRESTO (JPMJPR19T7) projects. We appreciate the technical staffs of the faculty of engineering, Hokkaido University and of Research Institute for Electronic Science, Hokkaido University for help with HAADF-STEM observation.

References

1. S. A. Nikolaev, V. V. Smirnov, A. Y. Vasil'Kov, V. L. Podshibikhin, *Kinet. Catal.*, 2010, **51**, 375-379.
2. M. Armbrüster, G. Wowsnick, M. Friedrich, M. Heggen, R. Cardoso-Gil*, J. Am. Chem. Soc.,* 2011, **133**, 9112-9118.
3. X. Liu, Y. Li, J. W. Lee, C.-Y. Hong, C.-Y. Mou, B. W. L. Jang, *Appl. Catal. A*, 2012, **439**, 8-14.
4. C. Ma, Y. Du, J. Feng, X. Cao, J. Yang, D. Li, *J. Catal.*, 2014, **317**, 263-271**.**
5. Y. He, Y. Liu, P. Yang, Y. Du, J. Feng, X. Cao, J. Yang, D. Li*, J. Catal.,* 2015, **330**, 61-70.
6. D. A. Lomeli-Rosales, M. D. Bernardos, S. Pèrez-Rodríguez, A. Gual, C. Claver, C. Godard, *Chem. Eur. J.*, 2019, **25**, 8321-8331.
7. Y. Liu, J. Zhao, Y. He, J. Feng, T. Wu, D. Li, *J. Catal.*, 2017, **348**, 135-145.
8. V. D. Stytsenko, D. P. Mel'nikov, O. P. Tkachenko, E. V. Savel'eva, A. P. Semenov, L. M. Kustov, *Russian Journal of Physical Chemistry A*, 2018, **92**, 862-869.
9. B. Bridier, J. Perez-Ramirez. *J. Am. Chem. Soc.,* 2010, **132**, 4321-4327.
10. S. Shoji, X. Peng, T. Imai, P. S. M. Kumar, K. Higuchi, Y. Yamamoto, T. Tokunaga, S. Arai, S. Ueda, A. Hashimoto, N. Tsubaki, M. Miyauchi, T. Fujita, H. Abe, *Chem. Sci.,* 2019, **10**, 3701-3705.
11. W. F. Simanullang, H. Itahara, N. Takahashi, S. Kosaka, K. Shimizu, S. Furukawa, *Chem. Commun.*, 2019, **55**, 13999-14002.
12. H. Ham. W.F. Simanullang, Y. Kanda, Y. Wen, A. Hashimoto, H. Abe, K. Shimizu, S. Furukawa, *ChemCatChem*, 2021, **13**, 1306-1310.
13. A. Borodziński, G. C. Bond, *Catal. Rev.: Sci. Eng.*, 2006, **48**, 91-144.
14. M. Armbrüster, K. Kovnir, M. Friedrich, D. Teschner, G. Wowsnick, M. Hahne, P. Gille, L. Szentmiklósi, M. Feuerbacher, M. Heggen, F. Girgsdies, D. Rosenthal, R. Schlögl, Y. Grin, *Nat. Mater.*, 2012, **11**, 690-693.
15. G. X. Pei, X. Y. Liu, A. Wang, A. F. Lee, M. A. Isaacs, L. Li, X. Pan, X. Yang, X. Wang, Z. Tai, K. Wilson, T. Zhang, *ACS Catal.*, 2015, **5**, 3717-3725.
16. C. Burda, X. Chen, R. Narayanan, M. A. El-Sayed, *Chem. Rev*., 2005, **105**, 1025-1102.
17. A. P. Alivisatos, *ACS Nano*, 2008, **2**, 1514-1516.
18. C. T. Campbell and J. Sauer, *Chem. Rev*., 2013, **113**, 3859-3862.
19. F. Studt, F. Abild-Pedersen, T. Bligaard, R. Z. Sorensen, C. H. Christensen, J. K. Norskov, *Science*, 2008, **320**, 1320-1322.
20. J. Hornung, M. Muhr, C. Gemel, R. A. Fischer, *Dalton Trans.*, 2019, **48**, 11743-11748.
21. H. Zhou, X. Yang, L. Li, Y. Huang, X. Pan, A. Wang, J. Li, T. Zhang, *ACS Catal.*, 2016, **6**, 1054-1061.
22. M. Miyazaki, S. Furukawa, T. Takayama, S. Yamazoe, T. Komatsu, *ACS Appl. Nano Mater*., 2019, **2**, 3307-3314.
23. J. van de Loosdrecht, A. M. van der Kraan, A. J. van Dillen, J. W. Geus, *Journal of Catalysis*, 1997, **170**, 217-226.
24. Z. Pan, R. Wang, J. Chen, *Appl. Cat. B: Environmental*, 2018, **224**, 88-100.
25. X. Meng, L. Wang, L. Chen, M. Xu, N. Liu, J. Zhang, Y. Yang, M. Wei, *J. Catal.*, 2020, **392**, 69-79.
26. S. Zhou, L. Kang, X. Zhou, Z. Xu, M. Zhu, *Nanomaterials*, 2020, **10**, 509.